Electronic Supplementary Material (ESI) for Physical Chemistry Chemical Physics

Supplementary Information for

Single-Molecule Conductance of Helical Peptides under Control of the Molecular Direction in a Molecular Junction

Hirotaka Uji, Tomoyuki Morita, and Shunsaku Kimura

Department of Material Chemistry, Graduate School of Engineering, Kyoto University, Kyoto-Daigaku-Katsura, Nishikyo-ku, Kyoto 615-8246, Japan

Tel: +81-75-383-2400 Fax: +81-75-383-2401 E-mail: shun@scl.kyoto-u.ac.jp

Materials

Synthesis of helical peptides. All chemicals were purchased from commercial suppliers and used without further purification. Ac-SA8S and SA8S-TMSE were synthesized by a conventional liquid-phase method. All the intermediates were identified by ^{1}H NMR spectroscopy (Bruker DPX-400) and the final products were further confirmed by FAB (JEOL JMS-HX110A) mass spectrometry. The purity of the intermediates was checked by thin-layer chromatography and the purity of the final compounds was checked by HPLC (TOSOH System 8020).

^{1}H NMR spectroscopy: hydrogen nuclear magnetic resonance spectroscopy

FAB mass spectrometry: fast atom bombardment mass spectrometry

HPLC: high-performance liquid chromatography

General procedures for the liquid-phase peptide coupling reactions. To a two-neck round bottom flask (RBF) filled with nitrogen gas were added a carboxyl acid component, an amine component, and DMF. The flask was cooled to 0 °C. A concentrated dimethyl formamide (DMF) solution of HATU was added to the mixture. HOAt was also added when the reaction rate is supposed to be slow. DIEA was then added to the mixture. The mixture was stirred at the designated temperature for the designated period under nitrogen atmosphere. The mixture was concentrated in reduced atmosphere. The residue was purified by one or combination of the following three methods: (1) taking up with chloroform ($CHCl_3$) and successive washes with 4 wt% aq $NaHCO_3$ (3×), brine, 4

wt% aq $KHSO_4$ (3×), and brine, followed by drying of the organic layer over Na_2SO_4; (2) purification by silica gel column chromatography; or (3) purification by Sephadex LH-20 chromatography.

HATU: 2-(7-aza-1H-benzotriazole-1-yl)-1,1,3,3-tetramethyluronium hexafluorophosphate

HOAt:1-hydroxy-7-azabenzotriazole

DIEA: *N*,*N*-diisopropylethylamine

N-terminal Linker

Thioacethyl Form

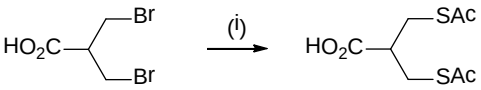

1 **2**

Disulfide Form

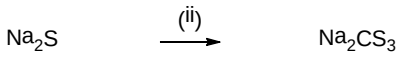

3 **4**

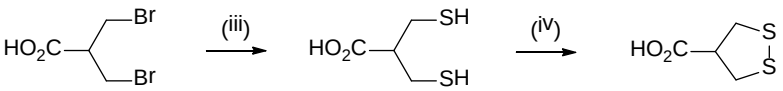

1 **5** **6**

C-terminal Linker

Trimethylsilylethyl Form

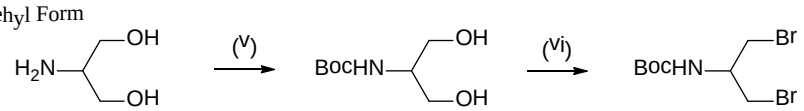

7 **8** **9**

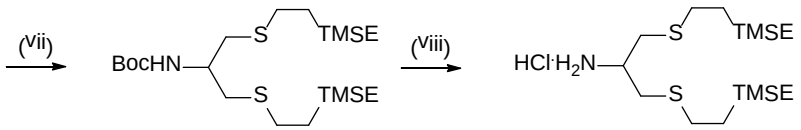

10 **11**

Disulfide Form

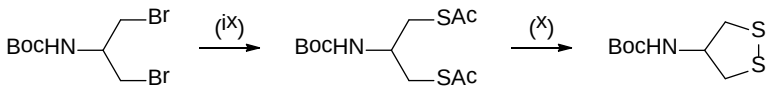

9 **12** **13**

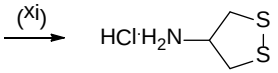

14

Scheme 1. Synthetic schemes of linkers. Reagents and conditions: (i) KSAc, DMF, 0 °C, 2 h; (ii) CS_2, water, reflux, 7 h, quant; (iii) Na_2CS_3 aq, reflux, 6 h, 66%; (iv) DMSO, 75 °C, 21 h, 55%; (v) Boc_2O, $CHCl_3$, 23 h, 98%; (vi) PPh_3, CBr_4, THF, 6 h, 56%; (vii) $TMSC_2H_4SH$, DBU, DMF, over night, 97%; (viii) HCl/Dioxane, 0 °C, 3 h, quant; (ix) KSAc, DMF, 0 °C, 2 h, 97%; (x) NH_4OH aq, MeOH, 24 h, 91% (xi) HCl/Dioxane, 1.5 h, quant.

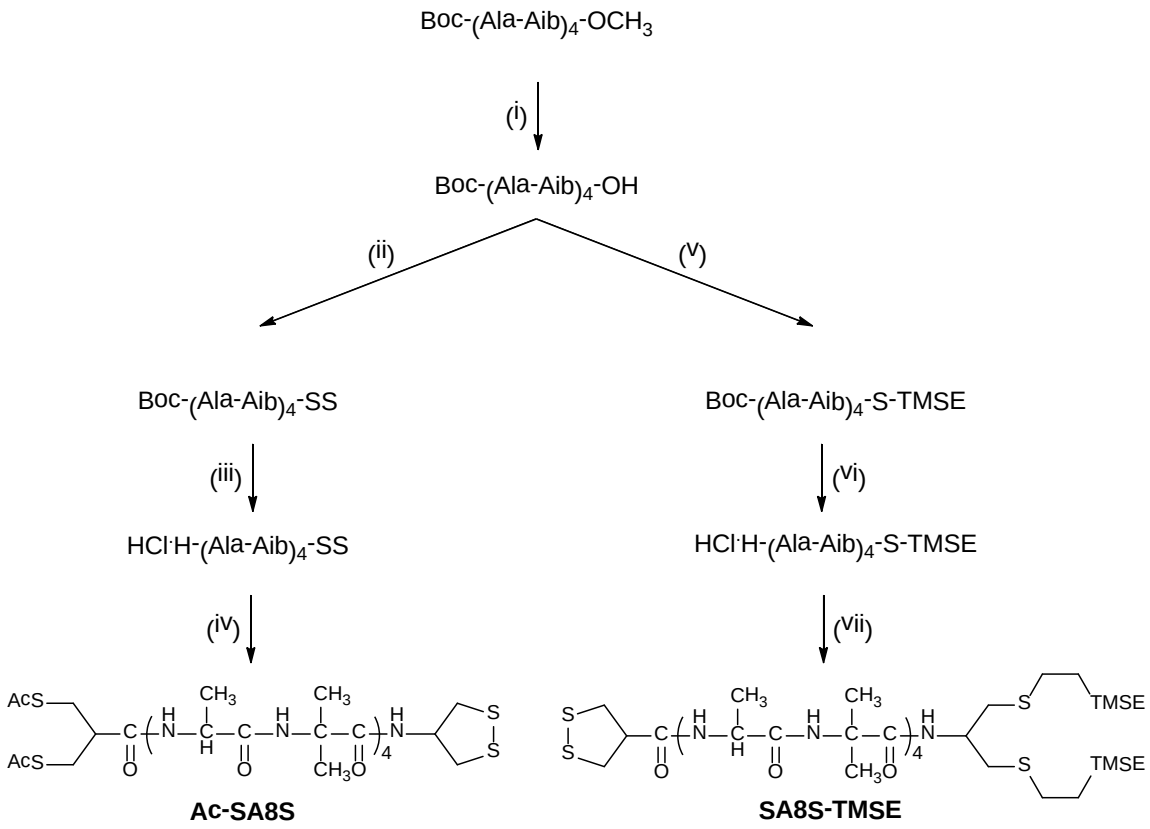

Scheme 2. Synthetic schemes of Ac-SA8S and SA8S-TMSE. Reagents and conditions: (i) NaOH aq, MeOH/Dioxane, 22 h, 79%; (ii) **13**, HATU, DIEA, DMF, 21 h, 82%; (iii) HCl/Dioxane, 1.5 h, quant; (iv) **2**, HATU, DIEA, DMF, 14 h, 8.5%; (v) **11**, HATU, HOAt, DIEA, DMF, 37 h, 88%; (vi) HCl/Dioxane; (vii) **6**, HATU, HOAt, DIEA, DMF, 14 h, 87%..

3-Acethylthio-2-(acethylthiomethyl)propionic acid (2)

To a well stirred solution of potassium thioacetate (2.22 g, 19.5 mmol) in dry DMF (30 mL) was added 3-bromo-2-(bromomethyl)propionic acid (2.00 g, 8.14 mmol) at 0 ^{o}C. After an additional 4 h of stirring at 0 ^{o}C under nitrogen atmosphere, the reaction mixture was taken up with ethyl acetate (EtOAc) and washed successively with 1 N aq HCl (3×), reextracted with ethylacetate (3×). The organic layer was dried over Na_2SO_4, concentrated under reduced pressure. The residue was purified by column chromatography (silica gel, eluent: $CHCl_3$/MeOH = 100/1 v/v) to obtain the product **2** as

yellow oil (1.92 g, 8.14 mmol, quant).

^{1}H NMR (400 MHz, $CDCl_3$) δ (ppm): 1.36 (6H, s, SCOCH_3), 2.92 (1H, m, C*H*COOH), 3.19 (4H, m, (AcSCH_2)$_2$CH).

3-Mercapto-2-(mercaptomethyl)propionic acid (5)

Sodium sulfide nonahydrate (**3**, $Na_2S{\cdot}9H_2O$, 38.2 g, 160 mmol) was added to water (100 mL). Carbon disulfide (CS_2, 11.6 mL, 192 mmol) was added to the aqueous solution of Na_2S at room temperature and kept stirring under reflux for 7 h at 50 ^{o}C. The remaining CS_2 was removed under reduced pressure. The residue was diluted with water to afford an aqueous solution of sodium trithiocarbonate (**4**, Na_2CS_3, 1 M, 160 mL). **4** (1 M, 60 mL) was added to 3-bromo-2-(bromomethyl)propionic acid (**1**, 4.91 g, 20.0 mmol) at room temperature under nitrogen atmosphere, and kept stirring under reflux for 6 h at 50 ^{o}C. After acidification with sulfuric acid (6 N), the reaction mixture was extracted with chloroform (3×). The organic layer was dried over $MgSO_4$, and concentrated under reduced pressure. The residue was recrystallized from cooled cyclohexane to afford **5** (2.01 g, 13.2 mmol, 66% yield).

TLC: R_f = 0.32 ($CHCl_3$/MeOH/AcOH=95/5/3 v/v/v). ^{1}H NMR (400 MHz, $CDCl_3$) δ (ppm): 1.51-1.55 (2H, t, S*H*), 2.81-3.00 (5H, m, (HSCH_2)$_2$C*H*COOH).

1,2-Dithiolane-4-carboxylic acid (6, asparagusic acid)

5 (1.88 g, 12.4 mmol) was added to dimethyl sulfoxide (DMSO, 20 mL), and kept stirring for 21 h

at 75 ^{o}C under nitrogen atmosphere. The reaction mixture was washed with cooled saturated aq $KHSO_4$, and extracted with cooled $CHCl_3$ (5×). The organic layer was dried over $MgSO_4$, concentrated under reduced pressure, purified by column chromatography (silica gel, eluent: $CHCl_3$/MeOH/AcOH = 100/1/1 v/v/v), and recrystallized from cyclohexane to afford **6** (1.02 g, 6.82 mmol, 55% yield).

TLC: R_f = 0.51 ($CHCl_3$/MeOH/AcOH = 95/5/3 v/v/v). ^{1}H NMR (400 MHz, $CDCl_3$) δ (ppm): 3.32-3.37 (2H, m, SSC*H*$_a$H$_b$CH), 3.47-3.54 (3H, m, SSCH$_a$*H*$_b$C*H*).

2-(*N*-*tert*-Butoxycarbonyl)amino-1,3-propanediol (8)

2-Amino-1,3-propanediol (**7**, 1.00 g, 11.0 mmol) and di-*tert*-butylcarbonate (2.97 g, 13.6 mmol) were added to $CHCl_3$ (174 mL) and the solution was stirred for 18 h at room temperature. The solvent was removed under reduced pressure and a crude product **8** was obtained (2.48 g, quant).

^{1}H NMR (400 MHz, $CDCl_3$) δ (ppm): 1.45 (9H, s, (C*H*$_3$)$_3$C), 2.64 (2H, s, O*H*), 3.68 (1H, br, NC*H*(CH$_2$OH)$_2$), 3.81 (4H, d, NCH(C*H*$_2$OH)$_2$), 5.23 (1H, br, N*H*)

2-(*N*-*tert*-Butoxycarbonyl)amino-1,3-dibromopropane (9)

To a well stirred solution of triphenylphosphine (9.88 g, 37.7 mmol) and **8** (3.00 g, 15.7 mmol) in dry tetrahydrofuran (THF, 3 mL) was added CBr_4 (12.5 g, 37.7 mmol) in small portions for 2 h at 0 ^{o}C. After an additional 23 h of stirring at room temperature, the precipitate was concentrated under reduced pressure. The residue was purified by column chromatography (silica gel, eluent:

$CHCl_3$/hexane = 1/1 v/v). 1.62 g of the desired product **9** (5.11 mmol, 32% yield) was obtained as a colerless crystal.

^{1}H NMR (400 MHz, $CDCl_3$) δ (ppm): 1.44 (9H, s, $(CH_3)_3C$), 3.52 (2H, m, $CHCH_aH_bBr$), 3.69 (2H, m, $CHCH_aH_bBr$), 4.09 (1H, br, $CHCH_aH_bBr$), 4.96 (1H, br, NH).

3-(*S*-2-Trimethylsilylethyl)thio-2-(*N*-*tert*-butoxycarbonyl)amino-propyl ethanethioate (10)

To a well stirred solution of 2-(trimethylsilyl)ethanethiol (202 μL, 1.26 mmol), **9** (100 mg, 315 μmol) in dry DMF (5 mL) was added DBU (240 μL, 1.58 mmol) at 0 ^{o}C. After an additional 12 h of stirring at room temperature, the reaction mixture was concentrated under reduced pressure. The residue was taken up with $CHCl_3$ and washed successively with 4 wt% aq $KHSO_4$ (2×), then dried over with Na_2SO_4. The crude product was purified by column chromatography (silica gel, eluent: hexane/EtOAc = 30/1 v/v) to obtain the product **10** as a colorless liquid (133 mg, 315 μmol, quant.).

^{1}H NMR (400 MHz, $CDCl_3$) δ (ppm): 0.00 (18H, $Si(CH_3)_3$), 0.85 (4H, $SiCH_2CH_2$), 1.43 (9H, s, $(CH_3)_3C$), 2.55 (4H, $SiCH_2CH_2$), 2.72-2.80 (4H, $CHCH_2STMS$), 3.88 (1H, br, $CHCH_2S$), 4.74 (1H, br, NH).

DBU: 1,8-Diazabicyclo[5.4.0]undec-7ene

TMSE: (*S*-2-Trimethylsilylethyl)thio

1,3-Diacetylthio-2-(*N*-*tert*-butoxycarbonyl)aminopropane (12)

To a well stirred solution of potassium thioacetate (2.93 g, 25.6 mmol) in dry DMF (30 mL) was

added **9** (2.90 g, 9.15 mmol) at 0 ^{o}C. After an additional 2 h of stirring at 0 ^{o}C under nitrogen atmosphere, the reaction mixture was concentrated under reduced pressure. The residue was taken up with EtOAc (200 mL) and washed successively with 4 wt% aq $KHSO_4$ (3×), with brine (3×) and reextracted with EtOAc (2×). The organic layer was dried over Na_2SO_4, concentrated under reduced pressure. The residue was purified by column chromatography (silica gel, eluent: $CHCl_3$/EtOAc = 100/1 v/v) to obtain the product **10** as a white solid (2.72 g, 8.86 mmol, 97% yield).

^{1}H NMR (400 MHz, $CDCl_3$) δ (ppm): 1.43 (9H, s, $(CH_3)_3C$), 2.36 (6H, s, $SCOCH_3$), 3.09 (4H, d, $CHCH_2S$), 3.88 (1H, br, $CHCH_2S$), 4.74 (1H, br, N*H*). FAB-MS m/z: $[M]^+$ calcd for $C_{12}H_{21}NO_4S_2$, 307.09; found, 307.

1,2-Dithiolane-4-(*N*-*tert*-butoxycarbonyl)amine (13)

To a well stirred solution of **12** (500 mg, 1.63 mmol) in MeOH (10 mL) was added 28% aq NH_4OH (10 mL). After an additional 8 h of stirring at room temperature under nitrogen atmosphere, the reaction solution was diluted with MeOH (150 mL). After an additional 15 h of stirring at room temperature under air, the reaction mixture was concentrated under reduced pressure and purified by column chromatography (silica gel, eluent: $CHCl_3$/EtOAc = 100/1 v/v). The desired product **13** (327 mg, 1.48 mmol, 91% yield) was obtained as a yellow solid.

^{1}H NMR (400 MHz, $CDCl_3$) δ (ppm): 1.46 (9H, s, $(CH_3)_3C$), 2.91 (2H, d, $CHCH_aH_bSS$), 3.60 (2H, d, $CHCH_aH_bSS$), 4.09 (1H, br, $CHCH_aH_bSS$), 5.91 (1H, br, N*H*). GCEI-MS m/z: $[M]^+$ calcd for

$C_8H_{15}NO_2S_2$, 221.05; found, 221.

GCEI-MS: Gas chromatography electron ionization-mass spectrometry

1,2-Dithiolan-4-amine hydrochloride (14)

To a well stirred solution of **13** (97.0 mg, 438 μmol) in dioxane (3 mL) was added 4 N HCl/dioxane (27 mL). After an additional 1.5 h of stirring at room temperature, the reaction mixture was concentrated under reduced pressure and the product was washed by $CHCl_3$ (2×) and diethyl ether. The crude product **14** was obtained as a white solid (69.0 mg, quant).

^{1}H NMR (400 MHz, DMF-d_7) δ (ppm): 3.59 (4H, s, CHCH_2SS), 3.80 (1H, br, CHCH_2SS), 9.20 (3H, s, NH_3^+CH). GCEI-MS m/z: $[M\text{-}HCl]^+$ calcd for $C_3H_7NS_2$, 121.00; found, 121.

Boc-(Ala-Aib)$_4$-SS (BA8S)

14 (15.4 mg, 97.7 μmol) was coupled to BA8OH (Boc-(Ala-Aib)$_4$-OH, 30.0 mg, 40.4 μmol) with addition of DIEA (33.0 μL, 188 μmol) and HATU (23.0 mg, 61.0 μmol) for 1 h at 0 ^{o}C under nitrogen atmosphere and thereafter for 17 h at room temperature. Then the solvent was removed under reduced pressure and the product was purified by column chromatography (Sephadex LH20, eluent: MeOH) and then the crude product was taken up with $CHCl_3$ and washed successively with 4 wt% aq $KHSO_4$, 4 wt% aq $NaHCO_3$ and brine. The product was recrystallized from diisopropyl ether to afford BA8S (25.4 mg, 30.0 μmol, 74% yield) as. a white solid.

^{1}H NMR (400 MHz, $CDCl_3$) δ (ppm): 1.4-1.6 (45H, (CH_3)$_3$C, AlaC$^\beta H_3$, AibC$^\beta H_3$), 3.0 (2H,

CHC*H*$_a$H$_b$SS), 3.3 (2H, CHCH$_a$*H*$_b$SS), 3.9- 4.2 (4H, AlaC$^{\alpha}$*H*), 4.6 (1H, C*H*CH$_a$H$_b$SS), 5.1-8.2 (9H, N*H*). FAB-MS m/z: $[M+H]^+$ calcd for $C_{36}H_{64}N_9O_{10}S_2$, 846.41; found, 846.4.

Boc: *tert*-Butoxycarbonyl

Ac-SA8S

The Boc group of BA8S (110 mg, 130 μmol) was deprotected by treating with 4 N HCl/dioxane (10 mL) after diluted in dioxane (1 mL). After an additional 1 h of stirring at room temperature, the reaction mixture was concentrated under reduced pressure to obtain the deprotected product HCl·HA8S. **2** (90.6 mg, 383 μmol) was coupled to HCl·HA8S with addition of DIEA (177 μL, 1.02 mmol) and HATU (219 mg, 575 μmol) for 1 h at 0 °C under nitrogen atmosphere and thereafter for 15 h at room temperature. Then the solvent was removed under reduced pressure and the residue was taken up with $CHCl_3$ (100 mL) and washed successively with 4 wt% aq $KHSO_4$ (3×), brine (3×) and reextracted with $CHCl_3$ (3×). The organic layer was dried over Na_2SO_4, concentrated under reduced pressure. The residue was purified by column chromatography (Sephadex LH20, eluent: $CHCl_3$/MeOH = 1:1 v/v) twice and purified by HPLC (eluent: $CHCl_3$). The product was recrystallized from diisopropyl ether to afford Ac-SA8S (10.5 mg, 10.9 μmol, 8.5% yield).

^{1}H NMR (400 MHz, $CDCl_3$) δ (ppm): 1.4-1.6 (36H, AlaC$^{\beta}$*H*$_3$, AibC$^{\beta}$*H*$_3$), 2.37, 2.41 (6H, s, SCOC*H*$_3$), 2.7-3.4 (9H, C*H*C*H*$_2$SAc, CHC*H*$_2$SS), 3.9- 4.2 (4H, AlaC$^{\alpha}$*H*), 4.6 (1H, C*H*CH$_2$SS), 6.7-7.4 (9H, N*H*). FAB-MS m/z: $[M]^+$ calcd for $C_{36}H_{63}N_9O_{10}S_2$, 963.37; found, 963.3.

Boc-(Ala-Aib)$_4$-S-TMSE (BA8S-TMSE)

The Boc group of **10** (133 mg, 315 μmol) was deprotected by treating with 4 N HCl/dioxane (10 mL) at 0 ^{o}C. After an addithional 2 h of stirring at room temperature, the reaction mixture was concentrated under reduced pressure to obtain the deprotected product **11**. **11** (100 mg, 278 μmol) was coupled to BA8OH (100 mg, 139 μmol) with addition of DIEA (120 μL, 590 μmol) and HATU (79 mg, 208 μmol) for 30 min at 0^{o}C under nitrogen atmosphere and thereafter for 17 h at room temperature. Then the solvent was removed under reduced pressure and the product was purified by column chromatography (Sephadex LH20, eluent: MeOH) and then the crude product was taken up with $CHCl_3$ and washed successively with 4 wt% aq $KHSO_4$ and brine. The product was recrystallized from diisopropyl ether to afford BA8S-TMSE (124 mg, 88% yield) as. a white solid

^{1}H NMR (400 MHz, $CDCl_3$) δ (ppm): 0.00 (18H, Si(CH_3)$_3$), 0.85 (4H, SiCH_2CH$_2$), 1.4-1.6 (45H, (CH_3)$_3$C, AlaC$^{\beta}H_3$, AibC$^{\beta}H_3$), 2.56 (4H, SiCH$_2$CH_2), 2.75-2.77 (4H, CHCH_2STMS), 3.9- 4.2 (5H, C*H*CH$_2$STMS, AlaC$^{\alpha}$*H*), 5.1-7.7 (9H, N*H*). FAB-MS m/z: $[M+H]^+$ calcd for $C_{46}H_{89}N_9NaO_{10}S_2Si_2$, 1048.57; found, 1048.6.

SA8S-TMSE

The Boc group of BA8S-TMSE (124 mg, 118 μmol) was deprotected by treating with 4 N HCl/dioxane (10 mL) after diluted in dioxane (1 mL). After an additional 1 h of stirring at room temperature, the reaction mixture was concentrated under reduced pressure to obtain the deprotected

product HCl·HA8S-TMSE. **6** (50.0 mg, 332 μmol) was coupled to HCl·HA8S-TMSE with addition of DIEA (154 μL, 0.89 mmol) and HATU (189 mg, 498 μmol) for 1 h at 0°C under nitrogen atmosphere and thereafter for 15 h at room temperature. Then the solvent was removed under reduced pressure and the residue was taken up with $CHCl_3$ (100 mL) and washed successively with 4 wt% aq $KHSO_4$ (3×), brine (3×) and reextracted with $CHCl_3$ (3×). The organic layer was dried over Na_2SO_4, and concentrated under reduced pressure. The residue was purified by column chromatography (Sephadex LH20, eluent: MeOH) twice. The product was recrystallized from diisopropyl ether to afford SA8S-TMSE (104 mg, 87% yield).

^{1}H NMR (400 MHz, $CDCl_3$) δ (ppm): 0.00 (18H, $Si(CH_3)_3$), 0.85 (4H, $SiCH_2CH_2$), 1.4-1.6 (36H, $AlaC^{\beta}H_3$, $AibC^{\beta}H_3$), 2.56 (4H, $SiCH_2CH_2$), 2.78-2.86 (4H, $CHCH_2STMS$), 3.28-3.60 (4H, $CHCH_2SS$), 3.77 (1H, $CHCH_2SS$), 4.03-4.15 (5H, $CHCH_2STMS$, $AlaC^{\alpha}H$), 6.9-7.6 (9H, NH). FAB-MS m/z: $[M+Na]^+$ calcd for $C_{45}H_{85}N_9NaO_9S_4Si_2$, 1102.49; found, 1102.5.

Circular dichroism (CD) spectroscopy. CD spectra of the peptides were measured on a CD spectropolarimeter (J-820, JASCO, Tokyo). The solvent was methanol which can be used for CD spectroscopy. The measurements were carried out with an optical cell of 0.1 cm optical path length at room temperature. The residue concentration was set to be 0.83×10^{-3} M for Ac-SA8S, and 0.74×10^{-3} M for SA8S-TMSE. The CD spectra of the peptides are shown in Figure S1. The CD spectrum show a negative peak at around 205 nm and a following broad shoulder at around 223 nm, which is a characteristic profile of a 3_{10}-helix.[1]

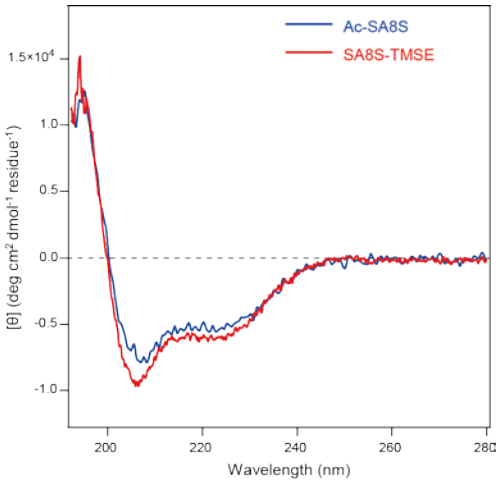

Figure S1. CD spectra of the peptides in methanol at ca. $0.74\text{-}0.83\times10^{-3}$ M residue concentration.

Preparation of self-assembled monolayers (SAMs). Gold substrates for infrared reflection-absorption spectroscopy (IRRAS) were prepared by following procedure. A glass slide (76 mm×5 mm) was cleaned with conc. sulfuric acid for 3 h, thoroughly rinsed with distilled water and methanol, and dried in vacuum for 15 min. A gold substrate was prepared by vapor deposition of

chromium (300 Å) and then gold (99.99%, 2000 Å) onto the glass slide by a vacuum deposition system (N-KS350, Osaka Vacuum, Osaka). The thickness of the chromium and gold layers were monitored by a quartz oscillator. The prepared gold substrate was immediately used for self-assembling. The peptide was dissolved in ethanol (ca. 0.1 mM). The gold substrate was then immersed in the solution for 24 h. After that, the substrate was rigorously rinsed with ethanol, ethanol/chloroform (1/1 v/v), and chloroform in this order, and dried with a nitrogen stream and in vacuum for 15 min. After the preparation, the monolayer samples were immediately used for the characteristic measurements.

Gold substrates for scanning tunneling microscopy (STM) and scanning tunneling spectroscopy (STS) were deposited on the surface of freshly cleaved mica by thermal evaporation (1000 Å) and then were annealed just before preparation of the SAMs. The freshly-prepared gold substrate was incubated in a solution of the peptide by the same procedure for samples for IRRAS. After the immersion and rinse, the peptide monolayers were treated in advance with a basic solution to remove protected groups. Ac-SA8S SAM was treated with a solution of ammonia water (28 wt%) in ethanol to cleave the acetyl group.[2] SA8S-TMSE SAM was treated with a solution of 5 mM tetrabutylammonium fluoride (TBAF) in THF to cleave the TMSE group.[3] The substrates were finally washed thoroughly with ethanol and dried in a stream of dry nitrogen gas. After the preparation, the monolayer samples were immediately used for the STM and STS measurements.

Molecular modeling. Molecular modeling was performed to determine the cross-sectional area of the helical peptide on a Fujitsu CAChe WorkSystem 6.1.1 software. The initial geometry of a model 8mer peptide lacking disulfide group and chromophore at the terminals was generated, in which the dihedral angles of the peptide backbone were set to be ω=180°, ϕ=-60°, and ψ=-30°, respectively, to produce a 3_{10}-helical structure.[4,5] The initial geometry was then optimized by the Molecular Mechanics program 2 (MM2) method and the semiempirical Austin Model 1 (AM1) method in the MOPAC 2002 package on the same software. The cross-sectional area of the helical peptide was estimated to be 0.69 nm^2 (9.4 Å diameter). The limiting surface density of helical peptide is estimated as 21.7×10^{-11} mol/cm^2, assuming hexagonal packing with a tilt angle of 0°. The theoretical surface densities were estimated by (limiting surface density)×cosγ, where γ is the tilt angle of helical axis from the surface normal.

The thicknesses of the monolayers were estimated by (molecular length)×cosγ. The molecular lengths of the peptides were calculated by the helix length and the length of the rest parts. The helix lengths were estimated with 2.0 Å per residue for a 3_{10}-helix[6] to be 16 Å. Since the conformation of the parts other than the helix is unknown, the half of the length of the longest extended conformation was used as approximation. The longest length was determined by geometry optimization of virtual condensation compounds of compound **2** and **14** in Scheme 1 for Ac-SA8S, and compound **6** and **11** for SA8S-TMSE, by the MM2 and AM1 method to be ca. 12 Å for Ac-SA8S and 13 Å for

SA8S-TMSE. Therefore, the molecular length is 22 Å for Ac-SA8S and 23 Å for SA8S-TMSE.

IRRAS measurements. The IRRAS spectra of the peptide monolayers on gold were recorded on a Nicolet Magna 850 Fourier transform infrared spectrometer with a Harrick RMA-1DG/VRA reflection attachment at room temperature. The incident light is not polarized and its incident angle was set at 84º from the surface normal. The number of interferogram accumulations was 200. The molecular orientation of the helical peptide was determined from of the amide I/amide II absorbance ratio in the IRRAS spectrum according to eq. 1 under the assumption of uniform orientation of the helix axis around the surface normal.[7,8]

$$I_1 / I_2 = 1.5 \left((3\cos^2\gamma\text{-}1) (3\cos^2\theta_1\text{-}1) +2\right) / \left((3\cos^2\gamma\text{-}1) (3\cos^2\theta_2\text{-}1) +2\right) \qquad (1)$$

I_i, γ, and θ_i (i=1 or 2 corresponding to amide I or amide II) represent the observed absorbance, the tilt angle of helical axis from the surface normal, and the angle between the transition moment and the helix axis, respectively. The values of the θ_1 and θ_2 were taken to be 39º and 83º, respectively, for 3_{10}-helical conformation.[9,10]

Figure S2 shows IRRAS spectra of SAMs. The tilt angles of the helix axis from the surface normal were calculated to be 60° for the Ac-SA8S SAM and 45° for the SA8S-TMSE SAM. The monolayer thicknesses are calculated as 11 Å for the Ac-SA8S SAM and 16 Å for the SA8S-TMSE SAM. The theoretical surface densities are 10.9×10^{-11} mol/cm^2 for the SA8S-TMSE SAM and 15.3×10^{-11} mol/cm^2 for the SA8S-TMSE SAM.

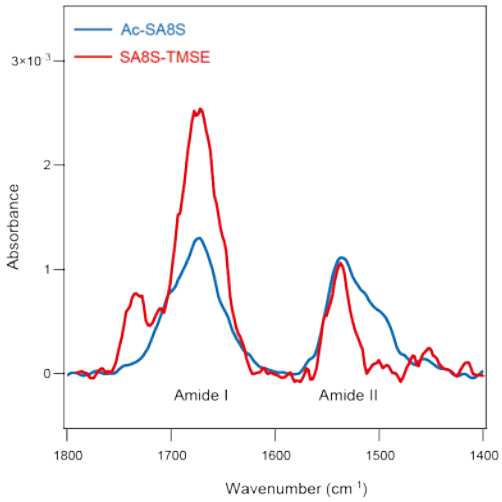

Figure S2. IRRAS spectra of SAMs: (blue) Ac-SA8S; (red) SA8S-TMSE.

Ellipsometry. The thicknesses of the peptide monolayers on gold were determined by a MIZOJIRI DHA-OLX/S autoellipsometer at room temperature. A helium-neon laser of 632.8 nm was used as the incident light, and the incident angle was set at 65º. The thickness of the monolayer was calculated automatically by using an equipped program. In the calculation, the complex optical constant of the monolayer was assumed to be 1.50+0.00i. The thickness was obtained as the average on more than 5 different regions of the monolayer.

Cyclic voltammetry. Cyclic voltammograms were obtained with using a BAS model 604 voltammetric analyzer at room temperature. A standard three-electrode setup was used with the monolayer-modified substrate as the working electrode, Ag/AgCl in a 3 M NaCl aq. as the reference electrode, and a platinum wire as the auxiliary electrode in a glass vessel capped with a silicon-rubber lid. The solution was a 1 mM $K_4[Fe(CN)_6]$ in 1 M KCl aqueous solution prepared

with Milli-Q water (>18 MΩ cm), and it was deaerated with nitrogen gas for 15 min prior to the experiments. The applied potentials of the working electrode reported here are with respect to the reference electrode. The area of the working electrode exposed to the electrolyte solution was 0.9−1.1 cm^2. The uncompensated resistance of the cell, estimated by electrochemical impedance spectroscopy, was ca. 3−4 ohm. The sweep rate was set at 0.1 V s^{-1}. Figure S3 shows the results of the blocking experiments. The bare gold substrate shows redox peaks of ferricyanide/ferrocyanide couple clearly.

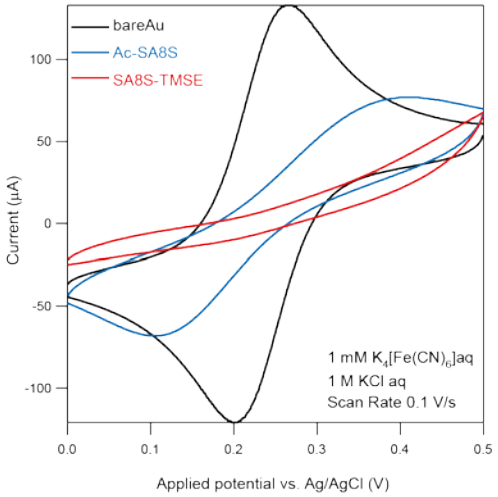

Figure S3. Cyclic voltammograms of a bare gold substrate and SAMs: (black) bare Au; (blue) Ac-SA8S; (red) SA8S-TMSE.

Table S1. Summary of monolayer characterization.

SAM	helical structure	tilt angle γ(°)	ellipsometry thickness (Å)	calculated thickness (Å)	theoretical surface density (×10^{-11} mol cm^{-2})	defects
Ac-SA8S	3_{10}-helix	60	9.1	11	10.9	moderate
SA8S-TMSE	3_{10}-helix	45	11.5	16	15.3	small

STM measurements. The STM measurements were performed with an Agilent 5500 SPM system. The STM tip was prepared by electrochemical etching of a 0.25 mm-diameter gold wire (99.999%) in conc. HCl aq./ethanol (1/1) with an AC voltage (15−22 V, 4 kHz). The etched wire was then cleaned with piranha solution, rinsed with ultrapure water, and dried in a nitrogen stream. The STM break-junction measurements were performed in toluene. The surface was first imaged in the constant current mode and the tip was placed within a large terrace on the monolayer. The feedback was then turned off when the tip located at the bias voltage, then the tip was automatically approached for 2 nm to the substrate and withdrawn for 6 nm repeatedly at a rate of 12.5 nm/s controlled by using an equipped program. The tip bias was kept at -0.1 V versus the substrate. The transient currents during the approach-withdraw repetition were recorded. The maximum current of current amplification was limited to be 1.0 nA for STM break-junction measurements and to be 10 nA for STS measurements. The measurements were carried out at different points on the sample, and the sample was tested at least two samples for each peptide. When every 500 curves were recorded, the tip was moved to an another large terrace on the monolayer. The number of the recorded curves was 10000-20000.

These curves were categorized into three types(see Figure 2A). The first type is an exponential decay by distance which is due to a junction in the absence of molecules. The second type is a noisy curve probably due to mechanical oscillations, ambient noise, or adsorbed molecules. These

two types of curves were rejected for histogram analysis. The last type is a curve with steplike features which are a proof of a formation of a gold-peptide(s)-gold junction. To calculate the conductance, current divided by the applied bias. The conductance histogram was based on the curves with plateau by the data points of a certain current versus the corresponding conductance. The histogram was then fitted with Gaussian curves to determine the average of the conductance.

Current-voltage curves were measured by using an equipped program. The STM tip was pleased within a terrace on the monolayer (set current: 0.2 nA, applied sample bias; -0.1 V). Then, the feedback electric circuit was cut off to fix the tip and sample distance during voltage sweeps. The bias voltage was applied to the sample with taking the grounded tip as zero. Bias voltage was swept separately from zero to +1.8 V and from zero to -1.8 V. More than 1000 scans of current-voltage curves were measured. Current-voltage curves with fluctuation of more than 10 nA, current response of less than 0.1 nA in the whole bias sweep, and no bias response were rejected for analysis.

Theoretical calculation. All of the first principle calculation were carried out using Gaussian 03[11] with B3LYP/6-31G+(d,p) level. The external electric field effect was calculated by "field" command of Gaussian 03. For the energy diagrams, the peptide is divided into four parts of linker-Ala, tripeptide, tripeptide, and Aib-linker from the calculated optimized conformation of whole peptide molecule (Figure S4A). The molecular orbitals of the each peptide moiety were calculated by the single point calculation. For calculation of the energy diagrams, we utilized the data in the

literature[12] in which the electrostatic potential by surface potential in the peptide monolayer was determined. The surface potential of monolayer V_{SAM} is described[13] as

$$V_{SAM} = \frac{\mu_{SAM}}{\varepsilon_0 \varepsilon_{SAM} A},$$

where μ is the actual value of the dipole moment normal to the substrate for a molecule, A the area occupied by each molecule, and ε_{SAM} the dielectric constant, ε_0 the permittivity of free space. In this formula, μ is calculated as 58.0×10^{-30} C m, ε_0 is 8.85×10^{-12} J^{-1} C^2 m^{-1}, ε_{SAM} is 3 for helical peptides according to the literature value,[12] A is evaluated as 1.38 nm^2, respectively. Then, the value of V_{SAM} was calculated as 1.6 V. Since the exact electronic coupling between each peptide moiety, this electrostatic surface potential applied to the molecular orbital energy of each peptide moiety in a linear gradient manner.

With applying a negative bias voltage to the C terminal, Au Fermi level of the right electrode was moves up and that of the left one moves down (Figure S4B blue line). The potential profile between two electrode was described as a blue dotted line, and light blue trigonal area are meaning a window of applied bias voltage. Under applying the electric field antiparallel to the dipole, the occupied molecular orbitals were calculated to move up (Figure 3B left), illustrated in Figure S4B as blue tilted line meaning upper limit of occupied molecular orbitals. In this energy diagram, the electronic coupling between two electrodes and occupied molecular orbitals including HOMO was illustrated as the deep blue area. Reversed applying the external electric field, Au Fermi level moves in the

opposite manner, and Figure 3B right shows the occupied molecular orbitals shift down (Figure S4C). More HOMO orbitals become available with applying a negative bias voltage to the C terminal than with a positive bias voltage, which is agreeable with the observed rectification behavior of the peptides.

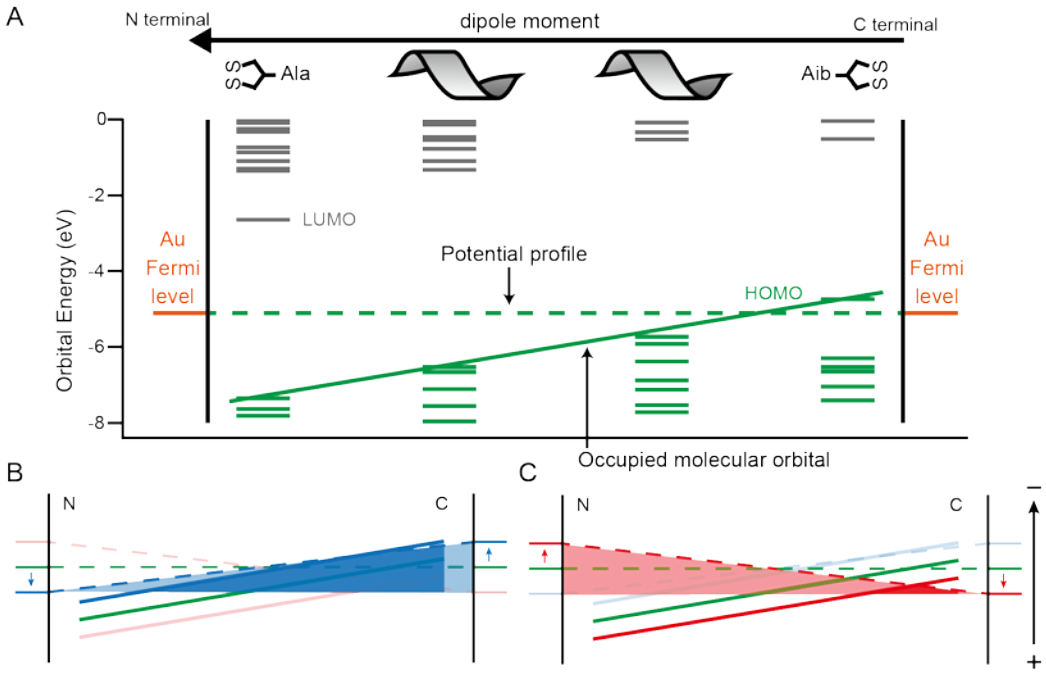

Figure S4. (A) Molecular fragmentation energy diagrams at the molecular junction. **(B)** Energy diagrams with applying a negative bias voltage, and **(C)** a positive bias voltage to the C terminal.

Reference.

(1) Toniolo, C.; Polese, A.; Formaggio, F.; Crisma, M.; Kamphuis, J. *J. Am. Chem. Soc.* 1996, *118*, 2744–2745.

(2) Kitagawa, K.; Morita, T.; Kimura, S. *Thin Solid Films* 2006, *509*, 18–26.

(3) Morales, G. M.; Jiang, P.; Yuan, S.; Lee, Y.; Sanchez, A.; You, W.; Yu, L. *J. Am. Chem. Soc.* 2005, *127*, 10456–10457.

(4) Császár, A. G.; Perczel, A. *Progress in Biophysics and Molecular Biology* 1999, *71*, 243–309.

(5) Santhanamoorthi, N.; Kolandaivel, P.; Senthilkumar, K. *J. Phys. Chem. A* 2006, *110*,

11551–11556.

(6) Benedetti, E.; Di Blasio, B.; Pavone, V.; Pedone, C.; Santini, A.; Crisma, M.; Toniolo, C. *Molecular Configuration and Biological Interactions*; Balaram, P.; Ramaseshan, S., Eds.; Eds. Indian Academy of Science: Bangalore, 1991.

(7) Gremlich, H. U.; Fringeli, U. P.; Schwyzer, R. *Biochemistry* 1983, *22*, 4257–4264.

(8) Miura, Y.; Kimura, S.; Imanishi, Y.; Umemura, J. *Langmuir* 1998, *14*, 6935–6940.

(9) Marchessault, R. H.; Liang, C. Y. *Journal of Polymer Science* 1962, *59*, 357–378.

(10) Kennedy, D. F.; Crisma, M.; Toniolo, C.; Chapman, D. *Biochemistry* 1991, *30*, 6541–6548.

(11) . Gaussian 03, Revision C.02, M. J. Frisch,_ G. W. Trucks, H. B. Schlegel, G. E. Scuseria, M. A. Robb, J. R. Cheeseman, J. A. Montgomery, Jr., T. Vreven, K. N. Kudin, J. C. Burant, J. M. Millam, S. S. Iyengar, J. Tomasi, V. Barone, B. Mennucci, M. Cossi, G. Scalmani, N. Rega, G. A. Petersson, H. Nakatsuji, M. Hada, M. Ehara, K. Toyota, R. Fukuda, J. Hasegawa, M. Ishida, T. Nakajima, Y. Honda, O. Kitao, H. Nakai, M. Klene, X. Li, J. E. Knox, H. P. Hratchian, J. B. Cross, V. Bakken, C. Adamo, J. Jaramillo, R. Gomperts, R. E. Stratmann, O. Yazyev, A. J. Austin, R. Cammi, C. Pomelli, J. W. Ochterski, P. Y. Ayala, K. Morokuma, G. A. Voth, P. Salvador, J. J. Dannenberg, V. G. Zakrzewski, S. Dapprich, A. D. Daniels, M. C. Strain, O. Farkas, D. K. Malick, A. D. Rabuck, K. Raghavachari, J. B. Foresman, J. V. Ortiz, Q. Cui, A. G. Baboul, S. Clifford, J. Cioslowski, B. B. Stefanov, G. Liu, A. Liashenko, P. Piskorz, I. Komaromi, R. L. Martin, D. J. Fox, T. Keith, M. A. Al-Laham, C. Y. Peng, A. Nanayakkara, M. Challacombe, P. M. W. Gill, B. Johnson, W. Chen, M. W. Wong, C. Gonzalez, and J. A. Pople, Gaussian, Inc., Wallingford CT, 2004.

(12) Jaworek, T.; Neher, D.; Wegner, G.; Wieringa, R. H.; Schouten, A. J. *Science* 1998, *279*, 57–60.

(13) Saito, N.; Hayashi, K.; Sugimura, H.; Takai, O.; Nakagiri, N. *Chemical Physics Letters* 2001, *349*, 172–177.